

# Resonance decay effects on anisotropy parameters

X. Dong<sup>a,b</sup>, S. Esumi<sup>c</sup>, P. Sorensen<sup>b</sup>, N. Xu<sup>b</sup>, Z. Xu<sup>d</sup>

<sup>a</sup>Department of Modern Physics, University of Science and Technology of China, Hefei, 230026, China

<sup>b</sup>Nuclear Science Division, Lawrence Berkeley National Laboratory, Berkeley, CA 94720, USA

<sup>c</sup>Institute of Physics, University of Tsukuba, Tsukuba, Ibaraki 305, Japan

<sup>d</sup>Physics Division, Brookhaven National Laboratory, Upton, NY 11973, USA

We present the elliptic flow  $v_2$  of pions produced from resonance decays. The transverse momentum  $p_T$  spectra of the parent particles are taken from thermal model fits and their  $v_2$  are fit under the assumption that they follow a number-of-constituent-quark (NCQ) scaling law expected from quark-coalescence models. The  $v_2$  of pions from resonance particle decays is found to be similar to the measured pion  $v_2$ . We also propose the measurement of electron  $v_2$  as a means to extract open-charm  $v_2$  and investigate whether a thermalized system of quasi-free quarks and gluons (a quark-gluon plasma) is created in collisions of Au nuclei at RHIC.

*Introduction.*—One of the surprising observations made at RHIC is the measurement of a number-of-constituent-quark (NCQ) dependence for both elliptic flow  $v_2$  and the nuclear modification factor  $R_{CP}$  at intermediate  $p_T$  ( $1.5 < p_T < 5$  GeV/c) [1]. Models of hadron formation by constituent-quark coalescence provide a viable explanation for these observations whereas expectations based on conventional fragmentation approaches are inconsistent with the data [2–4]. In coalescence models an NCQ-scaling of  $v_2$  arises as a consequence of hadrons coalescing out of a thermal distribution of partons and reveals the flow developed during a partonic epoch at RHIC. Pion  $v_2$ , however, appears to violate NCQ-scaling. In this paper, we study the effect of resonance decays on pion  $v_2$ . We show that when decays are taken into account, the measured pion  $v_2$  may become consistent with the NCQ-scaling demonstrated by the kaon ( $K^+$ ,  $K^-$ ,  $K_S^0$ ), proton,  $\Lambda$ , and  $\Xi$   $v_2$  distributions [1,5].

The particle azimuthal distribution with respect to the reaction plane at rapidity  $y$  can be described by a Fourier expansion:

$$\frac{dN}{d\Delta\phi} \propto 1 + \sum_n 2v_n \cos(n\Delta\phi), \quad (1)$$

where  $\Delta\phi$  is the difference in azimuth angle between the particle and the reaction plane. The first and second Fourier coefficients,  $v_1$  and  $v_2$ , historically are called directed and elliptic flow, respectively. All coefficients can be calculated from the relation:  $v_n = \langle \cos(n\Delta\phi) \rangle$ .

As the volume of the system created in an off-axis nucleus-nucleus collision expands, its spatial anisotropy quenches. The momentum-space anisotropies represented by the Fourier coefficients  $v_n$  preserve information about the early collision dynamics when the spatial anisotropy was largest [2,6–8]. Since the initial overlap region is elliptical in shape, the second harmonic coefficient  $v_2$  is the largest and most studied.

*NCQ-scaling of  $v_2$ .*—Fig. 1 shows the  $\pi^- + \pi^-$ ,  $K_S^0$ ,  $p + \bar{p}$ , and  $\Lambda + \bar{\Lambda}$   $v_2$  from minimum-bias  $^{197}\text{Au} + ^{197}\text{Au}$  collisions at  $\sqrt{s_{NN}} = 200$  GeV [1,5]. In the lower  $p_T$  region ( $p_T < 1.0$  GeV/c), the values of  $v_2$  are lower for higher mass hadrons. Hydrodynamic calculations [9] predict the observed mass dependence of  $v_2$ —perhaps implying that a thermalized system has been created in collisions at RHIC energy. At higher  $p_T$  ( $p_T \geq 2$  GeV/c), the  $v_2$  measurements saturate at values below the hydrodynamic model predictions. The saturated value of  $v_2$  and the  $p_T$  scale where

the saturation sets in depends on the particle-type: the baryon  $v_2$  saturates at higher  $p_T$  and at larger values than that of mesons.

According to coalescence models [4], after scaling both  $v_2$  and  $p_T$  with the number of the constituent quarks (NCQ) in the corresponding hadron, all particles at intermediate  $p_T$  should fall onto one universal curve. The NCQ-scaled  $v_2$  measurements in Fig. 1-(b) show that  $v_2/n_q(p_T/n_q)$  for  $p_T/n_q > 0.7$  GeV/c is similar for all particles *except* pions. This observation, coupled with the NCQ-dependence observed at intermediate  $p_T$  in the nuclear modification factor  $R_{CP}$  is evidence of hadron formation by coalescence or recombination. In this case,  $v_2/n_q(p_T/n_q)$  represents a constituent quark momentum-space anisotropy  $v_2^q$  that arises as a consequence of collectivity in a partonic stage. Based on coalescence models, NCQ-scaling suggests the creation of a quark-gluon plasma (QGP) with  $v_2^q$  characterizing the properties of the QGP. For this reason, understanding the source of the discrepancy in the NCQ-scaled pion  $v_2$  is imperative.

With this goal in mind, we study the effect of secondary pions (from particle decays) on the measured pion  $v_2$ . We assume that NCQ scaling is valid for all hadrons other than pions and use the published  $v_2$  measurements [1,5] to parameterize  $v_2/n_q(p_T/n_q)$ . The  $p_T$  distributions are assumed to follow an exponential form with slope parameters taken from measurements when available. We use chemical fits to fix the relative hadron abundances [10,11]. Since the pion mass is much smaller than the sum of its constituent quarks masses, direct pions are not necessarily assumed to follow the scaling predicted from coalescence models. As such, we do not consider direct pions, and instead choose to study the  $v_2$  of the secondary pions. Given the model uncertainties, extraction of the direct pion  $v_2$  is difficult and remains an open question. Finally we will discuss how to extract open-charm  $v_2$  based on the decayed electrons.

*Simulation results.*—The  $v_2$  values of the simulated resonances are parameterized by fitting  $K_S^0$

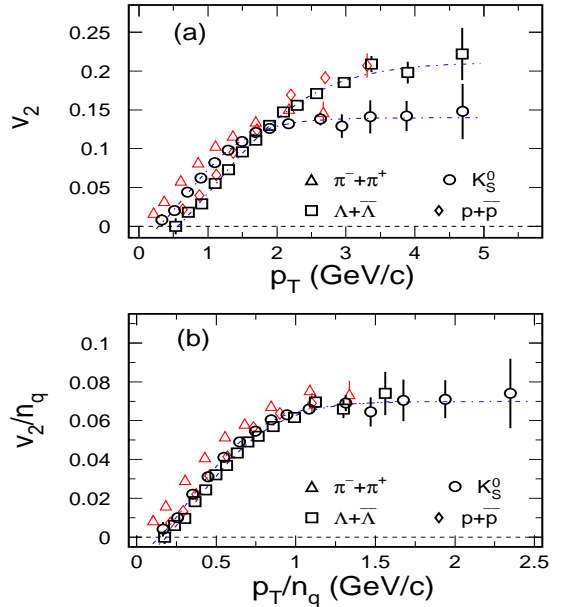


Figure 1. (a) Measurements of the  $p_T$  dependence of the event anisotropy parameters for  $\pi$ ,  $K_S^0$ ,  $p$ ,  $\Lambda$ . Dot-dashed lines are the results of fits; (b) Number-of-constituent-quark (NCQ) scaled  $v_2$ . All particles except the pions follow the NCQ scaling.

and  $\Lambda$   $v_2$  [1] with the equation:

$$f_{v_2}(n) = \frac{an}{1 + \exp(-(p_T n - b)/c)} - dn, \quad (2)$$

where  $a, b, c$  and  $d$  are the fit parameters and  $n$  is the constituent-quark number. The fit results are shown as dot-dashed lines in Fig. 1, where the fitting parameters are  $a = 0.1$ ,  $b = 0.35$ ,  $c = 0.2$  and  $d = 0.03$ . The NCQ-scaling of  $v_2$  works well for Kaons, protons and Lambdas within  $0.5 \leq p_T/n_q \leq 1.5$  GeV/c whereas pion  $v_2$  deviates from NCQ scaling for all  $p_T$ . The parameters from chemical fits are listed in Table 1.

In high-energy collisions, a large fraction of hadrons are produced through resonance decays. This is particularly true for pions in high-energy heavy-ion collisions. At mid-rapidity, in collisions

Table 1

Parameters for the input resonances: slope parameters  $T$  units are GeV. The fraction of the hadrons are fixed from the measured abundances.

	T1	T2	T3	Fraction (%)
$\rho$	0.5	0.4	0.3	$60 \pm 10$
$\omega$	0.5	0.4	0.3	$30 \pm 10$
$K_S^0$	0.3	0.3	0.3	$6 \pm 5$
$K^*(892)$	0.5	0.4	0.3	$2 \pm 1$
$\Delta$	0.55	0.55	0.55	$2 \pm 2$

at RHIC, as many as 80% of pions are from resonance decays [12]. The dominant decays are  $\rho \rightarrow \pi\pi$ ,  $\omega \rightarrow 3\pi$ ,  $K^*(892) \rightarrow K\pi$ ,  $K_S^0 \rightarrow \pi\pi$  and  $\Delta \rightarrow N\pi$ . With such a potentially large fraction of pions arising from decays, accounting for their effect on the observed pion  $v_2$  is very important.

The  $p_T$  distributions of pions from resonance decays are shown in Fig. 2. Most pions at  $p_T < 1$  GeV/c are generated from resonances with  $1 \leq p_T \leq 2$  GeV/c where  $v_2$  of the parent is near its maximum value. As a result the decayed pions take on a relatively large  $v_2$  value. The decays from the  $\rho$ - and  $\omega$ -mesons dominate the secondary pion  $p_T$  spectrum. In this plot, a slope parameter of  $T = 0.4$  GeV is used for the  $\rho$  distributions. In peripheral collisions, the STAR measured slope parameter is  $319 \pm 4(\text{stat.}) \pm 32(\text{syst.})$  MeV [13]. The simulated results are in a good agreement with the PHENIX  $\pi^0$  data from minimum bias  $^{197}\text{Au} + ^{197}\text{Au}$  collisions [14].

In Fig. 3, the  $v_2$  values for the simulated decay pions are shown as dashed-lines. The resonances included in this study are the  $\rho$ ,  $\omega$ ,  $K^*$ ,  $K_S^0$  and  $\Delta$ . The decay  $\rho \rightarrow \pi\pi$  with a 100% branching ratio dominates the production of secondary-pions. The simulated resonance particles are restricted to mid-rapidity  $|y| < 0.5$ . Increasing the rapidity window does not change the results. The pion  $v_2$  in the region  $p_T \leq 1.5$  GeV/c is sensitive to the shape of the  $\rho$   $p_T$  spectrum. Dashed-, dotted-, and dot-dashed-lines correspond to the  $v_2$  results from the different slope parameters listed in Table 1. For the smaller slope parameter  $T = 300$  MeV, the decayed pion  $v_2$  is below the data, leaving room for other contributions [15].

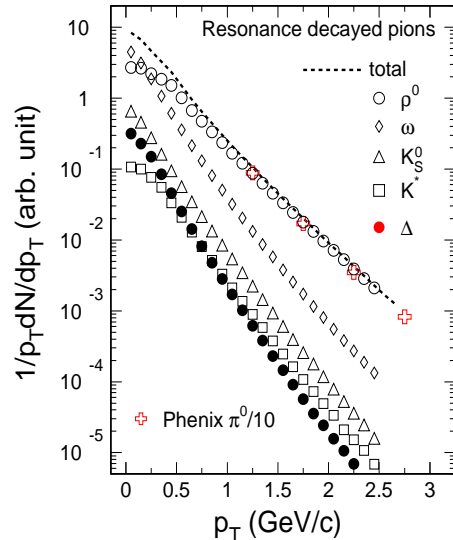


Figure 2. Resonance decayed pion distributions. The summed spectrum is shown as dashed-line. In this simulation, a slope parameter of  $T = 0.4$  GeV is used for  $\rho, \omega$  and  $K^*$ . For  $K_S^0$  and  $\Delta$  the respective slope parameters  $T = 0.3$  GeV and  $0.55$  GeV are used. The relative fraction of the hadrons are listed in Table 1. For comparison, PHENIX  $\pi^0$  results are shown as open-crosses.

*D-meson  $v_2$ .*—NCQ scaling suggests that hadrons at intermediate  $p_T$  are formed from a thermal partonic phase created in heavy-ion collisions at RHIC. In this system, the high initial matter density gradient and copious interactions among partons leads to a collective motion of partons. The large  $v_2$  values measured for multi-strange hadrons also indicate that partonic collectivity develops in collisions at RHIC [16]. Whether light flavored partons become thermalized, however, remains to be demonstrated. The development of collectivity for heavier partons should require much more re-scattering. As such, the measurement of heavy flavor (open-charm)  $v_2$  can probe the degree to which the lighter  $u$ -,  $d$ -, and  $s$ -quarks thermalize.

Since a large fraction of heavy-flavor hadrons

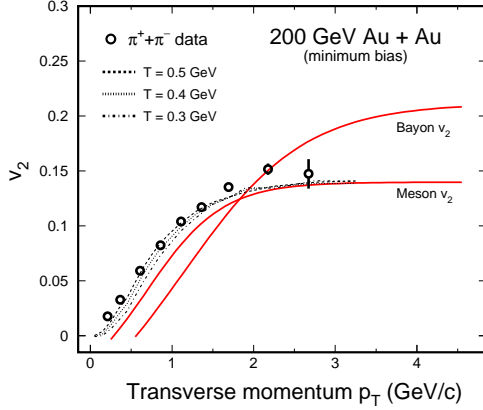


Figure 3. The measured pion  $v_2$  (symbols) is compared to the simulated  $v_2$  for pions from resonance decays (dashed lines). The assumed  $v_2$  of mesons and baryons are represented by the solid and dot-dashed lines, respectively.

decay through leptonic modes, electron  $v_2$  measurements may offer a convenient way to study open-charm  $v_2$ . In Fig. 4-(a), the  $v_2$  for electrons from D-meson decays is shown. Dot-dashed lines represent the assumed  $v_2$  of the parent meson. We simulate the D-meson  $p_T$  distribution using the PYTHIA event generator [17]. The shape of the calculated spectrum is well represented by a power-law function. Approximately 50 M D-meson events are used in this simulation. For electron  $p_T > 1.5$  GeV/c, the  $v_2$  of electrons from D-meson decays becomes similar to the parent D-meson  $v_2$ . The degree of heavy flavor thermal equilibrium can be assessed by measuring electron  $v_2$  within  $1 \leq p_T(e) \leq 3$  GeV/c a region which corresponds to  $\sim 2 \leq p_T(D) \leq 5$  GeV/c.

Neutral pion decays are the dominant source of “background” electrons. While the two-photon decay process,

$$\pi^0 \xrightarrow{\sim 100\%} \gamma + \gamma \xrightarrow{\text{few}\%} e^+ + e^- + e^+ + e^-,$$

can be identified by its decay topology [18], the pion Dalitz decay can only be subtracted statistically. In Fig. 4-(b) we show the  $v_2$  of electrons

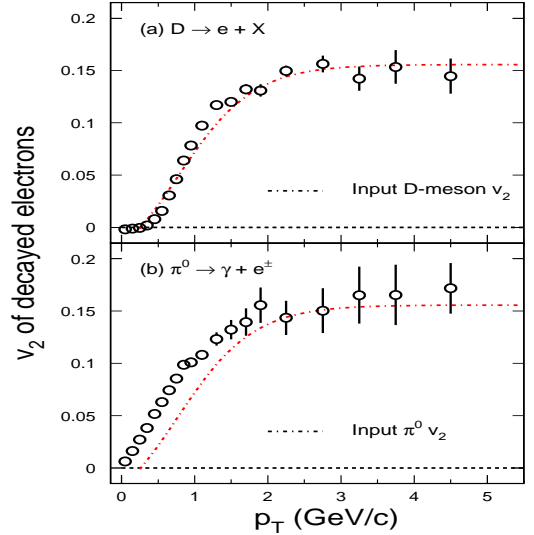


Figure 4. The  $v_2$  of electrons from D-meson decays (a) and  $\pi^0$  decays (b). The assumed input meson  $v_2$  curves are shown as dot-dashed lines in both plots.

from simulated pion Dalitz decays. The pion distribution can be obtained from measurements at RHIC [14]. For these simulations a 100% conversion probability is assumed. In STAR, however, the probability is closer to 5%. The decayed electrons predominantly have  $p_T \leq 0.5$  GeV/c [18].

Electrons from heavy flavor decays begin to dominate the electron spectrum above  $p_T \sim 3$  GeV/c. With knowledge of the pion yield, D-meson yield, the pion  $v_2$ , and the electron  $v_2$  it will be possible to extract the D-meson  $v_2$ . These measurements can be made by both the PHENIX and STAR collaborations at RHIC. Direct photon  $v_2$  can also be measured with this method.

*Summary.*—We have studied the effect of resonance decays on the pion  $v_2$  in Au+Au collisions at RHIC. When the  $v_2$  values for resonances are assumed to follow NCQ scaling, the pions generated in their decays take on  $v_2$  values similar to those measured at RHIC. The dominant source of secondary pions is  $\rho$  decays. We have shown that

when decays are accounted for, the measured pion  $v_2$  values *may* become consistent with the NCQ scaling law that suggests the development of partonic collectivity in collisions at RHIC. Model uncertainties, however, make it difficult to extract the direct pion  $v_2$ . In addition, we propose the measurement of electron  $v_2$  as a means to study open-charm  $v_2$  and hence the degree of thermalization reached at RHIC.

**Acknowledgements:** We appreciate fruitful discussions with P. Huovinen, C. Ko, H. G. Ritter, E. V. Shuryak, S. Voloshin. This work was supported in part by the NSFC under the Project No. 10275027 and the U.S. Department of Energy under Contract No. DE-AC03-76SF00098.

## REFERENCES

1. J. Adams *et al.* [STAR Collaboration], Phys. Rev. Lett. **92**, 052302 (2004).
2. S. A. Voloshin, Nucl. Phys. A **715**, 379 (2003).
3. R. J. Fries, B. Muller, C. Nonaka and S. A. Bass, Phys. Rev. C **68**, 044902 (2003).
4. Z. w. Lin and C. M. Ko, Phys. Rev. Lett. **89**, 202302 (2002); R. J. Fries, B. Muller, C. Nonaka and S. A. Bass, Phys. Rev. Lett. **90**, 202303 (2003); D. Molnar and S. A. Voloshin, Phys. Rev. Lett. **91**, 092301 (2003).
5. S. S. Adler *et al.* [PHENIX Collaboration], Phys. Rev. Lett. **91**, 182301 (2003).
6. H. Sorge, Phys. Lett. B **402**, 251 (1997).
7. J. Y. Ollitrault, Phys. Rev. D **46**, 229 (1992).
8. N. Xu and Z. b. Xu, Nucl. Phys. A **715**, 587 (2003).
9. P. Huovinen, P. F. Kolb and U. W. Heinz, Nucl. Phys. A **698**, 475 (2002); P. Huovinen, P. F. Kolb, U. W. Heinz, P. V. Ruuskanen and S. A. Voloshin, Phys. Lett. B **503**, 58 (2001).
10. P. Braun-Munzinger, K. Redlich and J. Stachel, arXiv:nucl-th/0304013 and references therein.
11. N. Xu and M. Kaneta, Nucl. Phys. A **698**, 306 (2002).
12. Z. b. Xu, J. Phys. G **30**, S325 (2004).
13. J. Adams *et al.* [STAR Collaboration], arXiv:nucl-ex/0307023.
14. S. S. Adler *et al.* [PHENIX Collaboration], Phys. Rev. Lett. **91**, 172301 (2003).
15. V. Greco and C. M. Ko, arXiv:nucl-th/0402020.
16. J. Adams *et al.* [STAR Collaboration], arXiv:nucl-ex/0307024.
17. T. Sjöstrand, L. Lönnblad and S. Mrenna, arXiv:hep-ph/0108264 and references therein.
18. I. J. Johnson [STAR Collaboration], Nucl. Phys. A **715**, 691 (2003).